Applied Thermal Engineering 29 (2009) 2518–2526

Contents lists available at ScienceDirect

Applied Thermal Engineering

journal homepage: www.elsevier.com/locate/apthermeng

Development of an air bleeding technique and specific duration to improve the CO tolerance of proton-exchange membrane fuel cells

Chen-Chung Chung *, Chiun-Hsun Chen, De-Zheng Weng

Department of Mechanical Engineering, National Chiao Tung University, 1001 University Road, Hsinchu, Taiwan 300, China

ARTICLE INFO

Article history:
Received 31 July 2008
Accepted 23 December 2008
Available online 30 December 2008

Keywords:
Proton-exchange membrane fuel cell
CO poisoning
Air bleeding technique
Catalyst

ABSTRACT

This study investigated transient CO poisoning of a proton-exchange membrane fuel cell under either a fixed cell voltage or fixed current density. During CO poisoning tests, the cell performance decreases over time. Experiments were performed to identify which method yields better performance in CO poisoning tests. The results revealed that a change in cell voltage did not affect the stable polarization behavior after CO poisoning of the cell. On the other hand, a higher fixed current density yielded better tolerance of 52.7 ppm CO. The air bleeding technique was then applied using different timings for air introduction during CO poisoning tests. Air bleeding significantly improved the CO tolerance of the cell and recovered the performance after poisoning, regardless of the timing of air introduction. The effects of different anode catalyst materials on cell performance were also investigated during poisoning tests. Without air bleeding, a Pt–Ru alloy catalyst exhibited better CO tolerance than a pure Pt catalyst. However, the air bleeding technique can effectively increase the CO tolerance of cells regardless of the type of catalyst used.

1. Introduction

The proton-exchange membrane fuel cell (PEMFC) is currently the focus of much attention because it runs at quite a low temperature, is highly efficient and quiet, and offers quick start-up. Therefore, PEMFCs are suitable for use in stationary and transportation applications. A PEMFC has an anode side, a cathode side, and a sandwich in between a solid polymer electrolyte membrane. Hydrogen and oxygen are fed into the anode and cathode, respectively. Platinum is the catalyst material predominantly used for anodes and cathodes because it exhibits high and stable activity for electro-oxidation of hydrogen and reduction of oxygen [1,2]. At the anode, hydrogen is oxidized into hydrogen ions and electrons. Protons diffuse through the membrane to reach the cathode, while electrons travel to the cathode, generating an electric current. Finally, hydrogen ions, electrons and oxygen at the cathode undergo a reduction reaction to generate water. Direct storage of hydrogen is difficult, so hydrocarbon fuels such as methanol, methane, and gasoline are passed through a fuel reformer to generate hydrogen for injection into fuel cell. However, the fuel reformer also produces a reformate gas containing carbon dioxide, carbon monoxide, and trace levels of other impurities. In fact, active adsorption of CO by the catalyst causes the Tafel reaction to become the rate-determining step and critically affects PEMFC performance. Dhar et al. [3] studied the effect of CO poisoning in PEMFC systems. They found that Pt catalysts were sensitive to poisoning by low levels of carbon monoxide. They also showed that the CO poisoning problem became much more severe at lower temperatures. Hence, the problem of CO poisoning needs to be solved for PEMFCs.

Many theoretical and experimental studies have addressed improvement of PEMFC CO tolerance. Various investigators have suggested techniques to reduce the effect of CO poisoning. These comprise increasing the ability to catalyze CO oxidation, weakening the adsorption of CO by the catalyst, and addition of an oxidant to the anode fuel stream to allow CO oxidation.

Replacing platinum as the anode catalyst by Pt–Ru alloys, such as Pt–Ru [4–7], Pt–Sn [8,9], and Pt–Mo [10,11], can improve the CO tolerance. Ham et al. [12] demonstrated that Pt supported on mesoporous tungsten carbide (WC phase) was an effective CO-tolerant electro-anode catalyst for hydrogen oxidation. A Pt/nanoporous WC catalyst showed twofold higher mass activity and much improved resistance to CO poisoning for hydrogen electro-oxidation compared to a commercial Pt/C catalyst.

Another way to improve CO tolerance is to feed an oxidant to the anode. The bleeding oxidant can be air or oxygen. A method for removing CO from the fuel cell involves feeding the fuel with a small amount of air or oxygen (air bleeding) [13–15]. Air bleeding into an impure anode fuel stream can generate an oxidative surface environment at the anode Pt catalyst, so CO is removed by oxidation to form CO_2. Thus, this technique is useful in improving CO

* Corresponding author. Tel.: +886 3 5712121x55180; fax: +886 3 5721091.
E-mail addresses: chenchung.me93g@nctu.edu.tw (C.-C. Chung), chchen@mail.nctu.edu.tw (C.-H. Chen), meddux.me91g@nctu.edu.tw (D.-Z. Weng).

1359-4311/$ - see front matter © 2009 Elsevier Ltd. All rights reserved.
doi:10.1016/j.applthermaleng.2008.12.021

tolerance. Shi et al. [16] reported that a PEMFC with a novel diffusion layer exhibited better performance than a traditional cell for a feed gas containing 100 ppm CO/H_2 and 2% air. The results revealed that Au particles in the diffusion layer were active in the water gas shift reaction at low temperature. Chu et al. [17] used air bleeding to overcome CO poisoning and applied the technique in a PEMFC stack. Chen et al. [18] reported that injection of 4% air was sufficient to restore fuel cell performance. They found that air dosing for 10 s at intervals of 10 s yielded a similar result to that for continuous air bleeding, except for 100 ppm CO. These results confirm that the CO tolerance of PEMFCs and performance recovery after poisoning can be improved by air bleeding.

In the present study, we investigated the improvement in PEMFC CO tolerance for the air bleeding technique. First, we defined suitable test poisoning conditions for PEMFCs that included fixing the cell voltage and the current density. The experimental results reveal which condition yields better CO tolerance and allow identification of the different parameters for the two methods. Second, we injected air into the anode fuel stream and investigated whether air bleeding could improve the PEMFC CO tolerance. Transient CO poisoning tests of long (30 min) or short duration (3 min) were applied. As the test duration was reached, air was injected into the anode fuel stream. The results were used to determine the air injection rate for a given CO concentration in the fuel stream that can effectively improve the CO tolerance and restore cell performance. Finally, we used a pure Pt catalyst to perform CO poisoning tests with and without air bleeding and the results were compared with those for a Pt–Ru alloy catalyst.

2. Fabrications and measurements

A PRIMEA series 5561 commercial membrane electrode assembly (MEA) from Gore was used in all fuel cell experiments in this study. Two-sided carbon paper backing with a thickness of 0.4 mm was used for the gas diffusion layer. The geometric active area of the membrane was 25 cm^2 and the cell border area was 100 cm^2. The MEA catalyst loads were 0.45 mg/cm^2 Pt–Ru alloy (1:1) on the anode and 0.6 mg/cm^2 Pt on the cathode. Graphite was used as the material for the flow field plates. A double-channel serpentine (with channel and rib widths of 0.1 cm each and a channel depth of 0.1 cm) was used for both the anode and cathode sites. The anode and cathode flows were co-current. The current collector was of gold-plated copper. The current collector board conducted electric current from the cell. Eight bolts were fastened into holes on one of the end plates, and the cell was compressed with a torque of 120 kgf cm.

The experimental conditions for these tests were fixed. The fuel flow rates for the anode and the cathode, determined from the theoretical volume flow rate that could generate 1 A, were 7.6 and 3.8 $cm^3\ min^{-1}\ A^{-1}$ for hydrogen and oxygen, respectively. The rate for the anode was multiplied by the stoichiometric ratio of 1.37 to yield a value of 10.4 $cm^3\ min^{-1}\ A^{-1}$, whereas that for the cathode was multiplied by 1.84 to yield 7 $cm^3\ min^{-1}\ A^{-1}$. The cathode stoichiometric ratio exceeds that of the anode because oxygen is less reactive. The backpressure on the anode and cathode sides was 1 atm. The cell temperature was held at 65 °C and the temperature of the anode and cathode humidifiers was held at 80 °C and 70 °C, respectively. These temperatures mean that the fuel is sufficiently humid to cross through the membrane, yielding optimum cell performance at the operating temperature of 65 °C. Table 1 summarizes the operational and experimental conditions used for the fuel cell.

The fuel cell test station consisted of an electronic load, MFC readout power supply, gas pipelines, controller, etc.

Table 1
Operational and experimental conditions.

Cell temperature	65 °C
Humidification temperature	Anode: 80 °C, cathode: 70 °C
Backpressure	Anode, cathode: 1 atm
Fuel flow rates	H_2: 10.4 $cm^3\ min^{-1}\ A^{-1}$
	O_2: 7 $cm^3\ min^{-1}\ A^{-1}$
Min. fuel flow rates	H_2: 104 $cm^3\ min^{-1}\ A^{-1}$
	O_2: 70 $cm^3\ min^{-1}\ A^{-1}$
Stoichiometry	H_2: 1.37, O_2: 1.84
Experiment 1	
Feeding fuel	Anode: H_2, H_2 + CO
	Cathode: O_2
Transient conditions	Fixed fuel cell voltage: 0.5, 0.6, and 0.7 V
	Fixed current density: 600, 1000, and 1200 mA/cm^2
CO concentration	52.7 ppm
Experiment 2	
Feeding fuel	Anode: H_2, H_2 + CO, H_2 + CO + air bleeding
	Cathode: O_2
Transient condition	Fixed current density: 800 mA/cm^2
CO concentration	10.1, 25, and 52.7 ppm
Air bleeding timing	30 and 3 min
Experiment 3	
Feeding fuel	Anode: H_2, H_2 + CO, H_2 + CO + air bleeding
	Cathode: O_2
Transient condition	Fixed current density: 800 mA/cm^2
CO concentration	52.7 ppm
Anode catalyst	Pt–Ru alloy and Pt
Air bleeding timing	30 min

3. Results and discussion

Transient CO poisoning experiments were first carried out under fixed cell voltage or fixed current density to identify which approach yields better CO tolerance. Then the timing effects of air bleeding during CO poisoning tests at fixed current density were investigated. Long (30 min) and short (3 min) poisoning durations were tested and compared. Finally, the effects of different catalysts (Pt and Pt–Ru) on CO poisoning tests with and without air bleeding were investigated.

3.1. Poisoning effects of fixed cell voltage and current density

In fixed voltage experiments, voltage values of 0.5, 0.6, and 0.7 V were tested. In experiments using a fixed current density, the settings chosen were 600, 1000, and 1200 mA/cm^2. In these tests, pure hydrogen was fed to the anode in the first 5 min, then changed to H_2/CO at a CO concentration of 52.7 ppm. The cell performance varied with time. Poisoned polarization curves were determined when the cell performance after poisoning reached a steady state.

3.1.1. Poisoning effects of fixed cell voltage

The results of CO experiments at fixed cell potential of 0.5, 0.6, and 0.7 V are shown in Fig. 1. In general, when the fuel was changed to H_2/CO, the cell performance in terms of the resultant current density decayed very quickly. This is because the operating temperature of the fuel is always maintained at 65 °C, at which CO has a stronger tendency than H_2 to adsorb onto the Pt catalyst. In other words, CO blocks active sites on the catalyst when present in the reaction chamber. Therefore, fewer active sites are available for hydrogen reaction, which decreases the cell performance.

As shown in Fig. 1, the current density decreased from 735 mA/cm^2 (pure H_2) to a stable value of 370 mA/cm^2 after 65 min of poisoning at 0.7 V. For a fixed cell voltage of 0.6 V, the current density decreased from 1460 mA/cm^2 (pure H_2) to

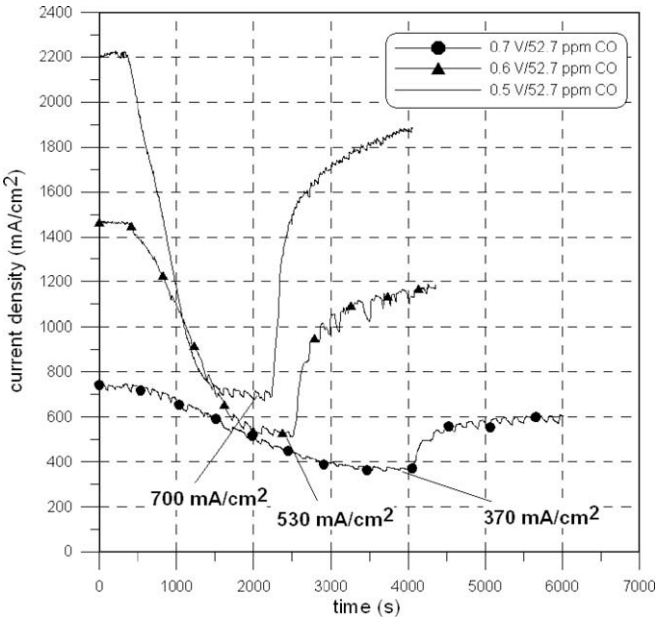

Fig. 1. CO poison and recovery performance at fixed cell potential.

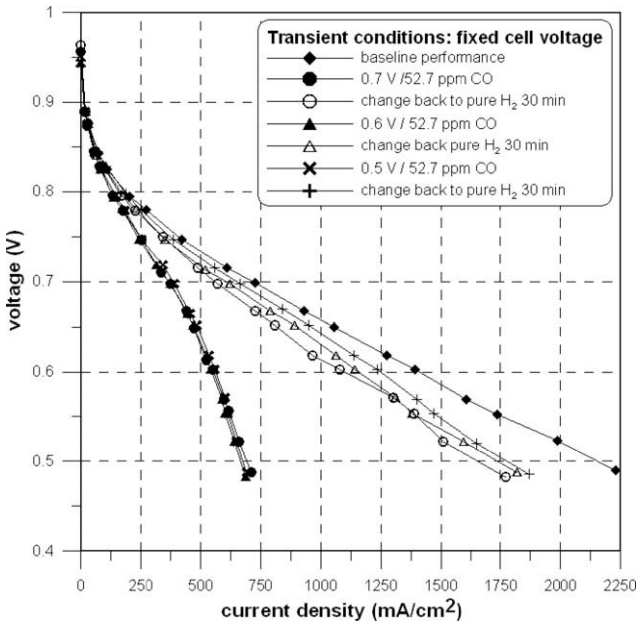

Fig. 2. Baseline, CO poison and recovery polarization curves for different CO poisoning conditions (0.5, 0.6 and 0.7 V).

530 mA/cm^2 after 40 min. For 0.5 V, the decrease was from 2200 to 700 mA/cm^2 after 35 min. These observations demonstrate that the decrease in performance was faster at the lower fixed voltage. A lower cell voltage produces a higher current density, which requires a higher fuel flow rate. Consequently, a higher amount of CO is supplied, leading to higher accumulation and adsorption of CO in the reaction chamber. Finally, competition between hydrogen and CO for adsorption on the Pt–Ru catalyst reaches a steady state. The time required to reach a steady state is mentioned above for each fixed voltage.

When a steady state was reached, the anode fuel was changed back to pure hydrogen, with no CO in the anode fuel stream. Adsorbed CO is then either desorbed from catalyst surface by hydrogen or oxidized at the Pt–Ru catalytic anode. The cell performance exhibited almost simultaneous recovery on introduction of pure hydrogen, as shown in Fig. 1. However, the recovery reached only ~80% of the original performance after 30 min of purging with pure hydrogen, indicating that CO was still adsorbed on active sites of the catalyst and could not be removed completely.

Fig. 2 shows baseline, poisoned and recovered polarization curves for different poisoning conditions (0.5, 0.6, and 0.7 V). It is significant that for a CO concentration of 52.7 ppm, the steady state poisoning polarization curves are almost coincident, regardless of the fixed voltage value chosen during CO tests carried out under the same conditions. This implies that at a given CO concentration, hydrogen and CO adsorption reactions on the Pt–Ru catalysts exhibit a fixed balance state or constant polarization behavior. The only difference observed was the duration required to reach the steady state.

Fig. 2 also shows that the recovery rate after purging with pure hydrogen was faster for lower cell voltage during CO tests. The reason is similar to that discussed for the poisoning effect observed in Fig. 1. At lower voltage the cell reaches a higher current density, which requires a higher fuel flow rate that may accelerate CO desorption from the catalyst. The other reason is that a low voltage induces CO oxidation, thus removing it from the catalyst. Therefore, CO experiments at a lower fixed voltage, such as 0.5 V, exhibited a better recovery rate (>85%) in Fig. 2. This explains the different polarization behaviors and performance recovery at different fixed voltages (0.5, 0.6, and 0.7 V).

3.1.2. Poisoning effects of fixed current density

Transient poisoning tests were also performed at different fixed current density. Fig. 3 shows cell voltage curves for fixed current density of 600, 1000, and 1200 mA/cm^2. In this case, cell performance, expressed as cell voltage, decayed very rapidly when the H_2/CO (52.7 ppm) fuel stream was introduced. CO introduction caused an increase in anode potential and a relative decrease in cell potential because CO adsorption blocked active sites on the catalyst. The performance after CO poisoning finally reaches a steady state, as shown in Fig. 3. For a fixed current density of 600 mA/cm^2 the cell voltage decayed from 0.725 V to a stable value of 0.550 V at 50 min after introduction of 52.7 ppm CO in the anode fuel stream. The voltage decay was from 0.662 V to 0.410 V after 45 min at 1000 mA/cm^2 and from 0.632 to 0.355 V after 30 min at 1200 mA/cm^2. Thus, a higher fixed current density resulted in a faster poisoning rate. The reason is same as that discussed for Fig. 1.

However, a slightly different phenomenon is evident between test carried out at fixed voltage and those at fixed current density. In the latter, the cell voltage sometimes exhibited oscillation after the poisoned performance reached a steady state, as shown in Fig. 3, whereas no such phenomenon was evident in tests at fixed voltage (Fig. 1). CO adsorption can increase the anode potential and a higher current density causes a higher anode potential. These effects quickly lead to the potential at which CO oxidation occurs, resulting in local CO removal from the catalyst and thus a slight recovery in cell voltage. Interaction between CO adsorption and oxidation reactions results in a feedback loop that causes the voltage oscillation observed.

Fig. 4 shows baseline, poisoned and recovered polarization curves for different poisoning conditions (600, 1000, and 1200 mA/cm^2). Better CO tolerance is evident when the cell is fixed at a higher current density (1200 mA/cm^2) during CO tests. In this case, CO poisoning is indicated by a decrease in cell voltage. CO poisoning always leads to an increase in anode potential and a decrease in overall cell performance. However, CO on the catalyst surface can take part in oxidative reactions if the anode potential reaches the onset potential for CO oxidation. CO oxidation over Pt–Ru catalysts occurs at an anode potential of approximately 0.2 V [9]. An anode potential greater than 0.2 V can increase the CO oxidation rate within a

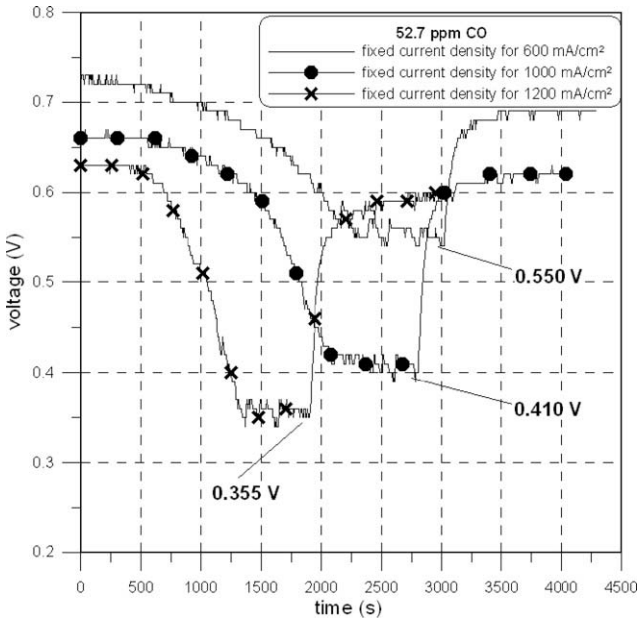

Fig. 3. CO poison and recovery performance at different fixed current density.

specific range. From Fig. 3, the increase in stable anode potential in the presence of 52.7 ppm CO at 600, 1000, and 1200 mA/cm^2 can be calculated as 0.175 V, 0.252 V, and 0.277 V, respectively. A higher anode potential causes a greater degree of CO removal from the catalyst surface, leading to better CO tolerance. Therefore, 1200 mA/cm^2 led to the best poisoned polarization performance at steady state (Fig. 4). On the contrary, a fixed cell voltage during poisoning tests may limit changes in the anode potential. Therefore, CO cannot be oxidized from the catalyst surface in the stable poisoned state. The stable values of CO adsorption are the same for all voltage conditions (0.5, 0.6, and 0.7 V), and the steady poisoned polarization behaviors are almost coincident.

For tests at fixed cell voltage, the discrepancy among stable polarization curves for different poisoning conditions was not significant and the anode polarization curves were very similar. The potential slope was higher than for test at fixed current density of 1000 and 1200 mA/cm^2. It can be concluded that changing the current density to a higher value can improve the CO tolerance but cannot change the stable poisoned polarization behavior during experiments at fixed cell voltage.

3.2. Effect of air bleeding timing

The effects of air bleeding on CO tolerance were investigated for specific air bleeding timings (3 and 30 min after poisoning was started) and different CO concentrations (10.1, 25, and 52.7 ppm). The current density was fixed at 800 mA/cm^2.

3.2.1. Long poisoning duration (30 min)

To determine the influence of air bleeding on CO tolerance, a stable baseline performance was first obtained after CO poisoning. Fig. 5 shows curves obtained at a fixed current density at 800 mA/cm^2 for poisoning tests at CO concentrations of 10.1, 25, and 52.7 ppm after an initial anode fuel stream of pure hydrogen in the first 5 min. The initial cell voltage for all tests was the same (0.701 V) in the first 5 min owing to the absence of CO poisoning. The cell voltage then decayed with time when CO was introduced into the fuel stream. The voltage reached a steady potential of 0.417 V for 52.7 ppm CO in 40 min, 0.476 V for 25 ppm CO in 85 min, and 0.588 V for 10.1 ppm CO in 3.5 h. Thus, the higher CO concentration, the faster were the poisoning and voltage decay rates. A higher CO concentration has a greater probability of blocking active sites on the catalyst surface and causing more serious CO poisoning. The curve for 52.7 ppm CO shows oscillating potential after the steady poisoned potential was reached. The anode potential may have reached the onset potential for CO oxidation in this situation. This would lead to CO desorption from the catalyst surface and thus a sudden recovery in cell voltage. The interaction between adsorption and desorption results in voltage oscillation. The 25 and 10.1 ppm CO curves reveal that the anode potential did not reach the onset potential for CO oxidation. Therefore, the cell voltage did not oscillate after reaching a steady state. The anode fuel was changed back to pure hydrogen when the steady state was reached (Fig. 5), after which the cell voltage recovered

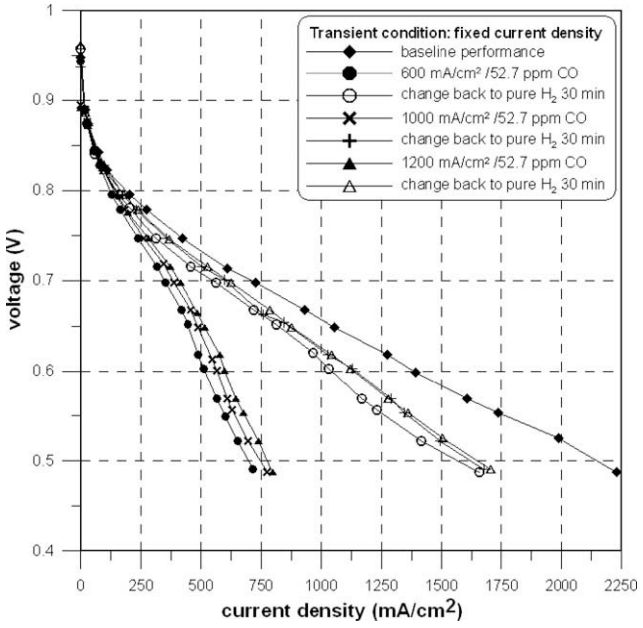

Fig. 4. Baseline, CO poison and recovery polarization curves for different poisoning conditions (600, 1000 and 1200 mA/cm^2).

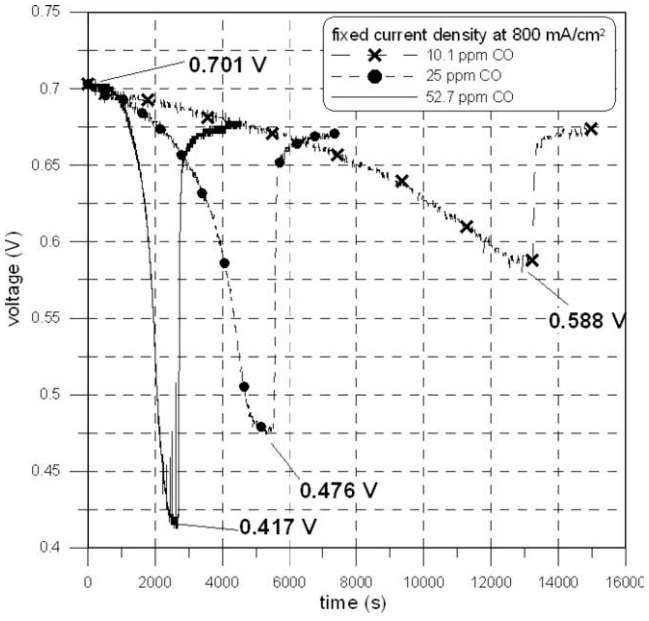

Fig. 5. Different concentrations of CO poisoning tests and recovery performance at a fixed current density at 800 mA/cm^2.

very quickly since CO was removed from the catalyst surface by pure hydrogen. The cell performance recovered to a value of ~0.675 V after purging with pure hydrogen for 30 min.

Fig. 6 shows steady polarization curves for different CO concentrations and the baseline curve for pure hydrogen. A higher CO poisoning concentration resulted in lower cell output. The cell power decreased to 0.223 W/cm^2 at 0.51 V for 52.7 ppm CO, representing only 20% of the baseline performance (1.163 W/cm^2). For 10.1 ppm CO, the power output decreased to 0.641 W/cm^2, which is half of the baseline value, at a cell potential of 0.51 V. Even the Pt–Ru alloy catalyst could not significantly decrease the CO poisoning for low CO concentrations. After purging with pure hydrogen for 30 min the polarization recovered to 80% of the baseline performance at 0.51 V.

The results for air bleeding during 30-min poisoning with 52.7 ppm CO are shown in Fig. 7a and b. In the initial 250 s. duration, a baseline by feeding pure hydrogen in this experiment was obtained to insure to reach a steady state. Then, impure hydrogen containing 52.7 ppm CO was fed to the anode. Air was introduced into the anode fuel stream after 30 min of CO poisoning. The initial cell potential was 0.701 V at a current density 800 mA/cm^2.

Fig. 7a is a plot of cell voltage versus time and shows the cell voltage recovery for different air bleeding ratios (2%, 3%, and 4%) in the anode fuel stream. The results indicate that the cell potentials recovered very quickly when air was introduced into the fuel stream after 30 min. The reason is that oxygen absorbs onto the catalyst and drives the oxidation reaction with CO to form CO_2. Therefore, CO is depleted from the catalyst surface and more of the active sites become available for hydrogen and further oxidation reactions. This leads to a decrease in anode potential and recovery of the cell potential. It is apparent that the air bleeding technique can improve the CO tolerance of PEMFCs. The rate of performance recovery also increased with the air ratio. The cell potential recovered to 0.681, 0.684, and 0.687 V for air bleeding ratios of 2%, 3%, and 4%, respectively. Moreover, it took approximately 15 min after air injection into the fuel stream for the cell potential to recover to a steady value.

Curves for air bleeding ratios from 2% to 8% are shown in Fig. 7b. The cell potential recovered to a constant value (0.687 V) even for an air ratio of 8%. An interesting phenomenon is that there was no further improvement in CO tolerance for air ratios greater than 4%.

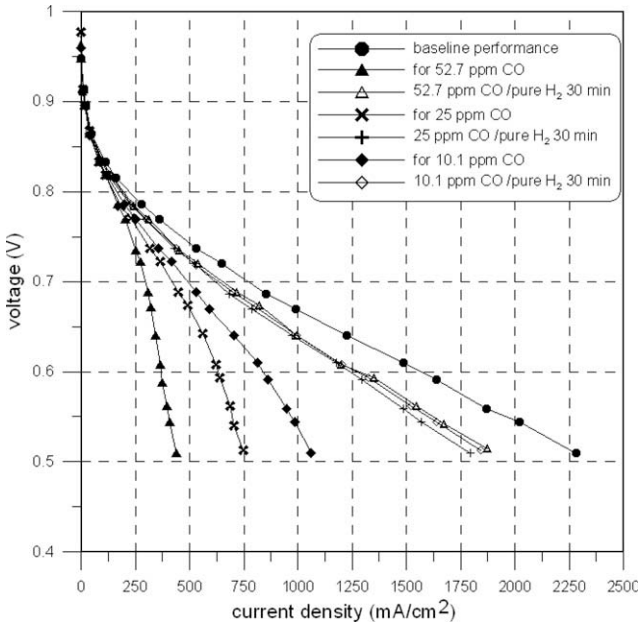

Fig. 6. Baseline, CO poison and recovery polarization curves for different CO poison conditions (600, 1000 and 1200 mA/cm^2).

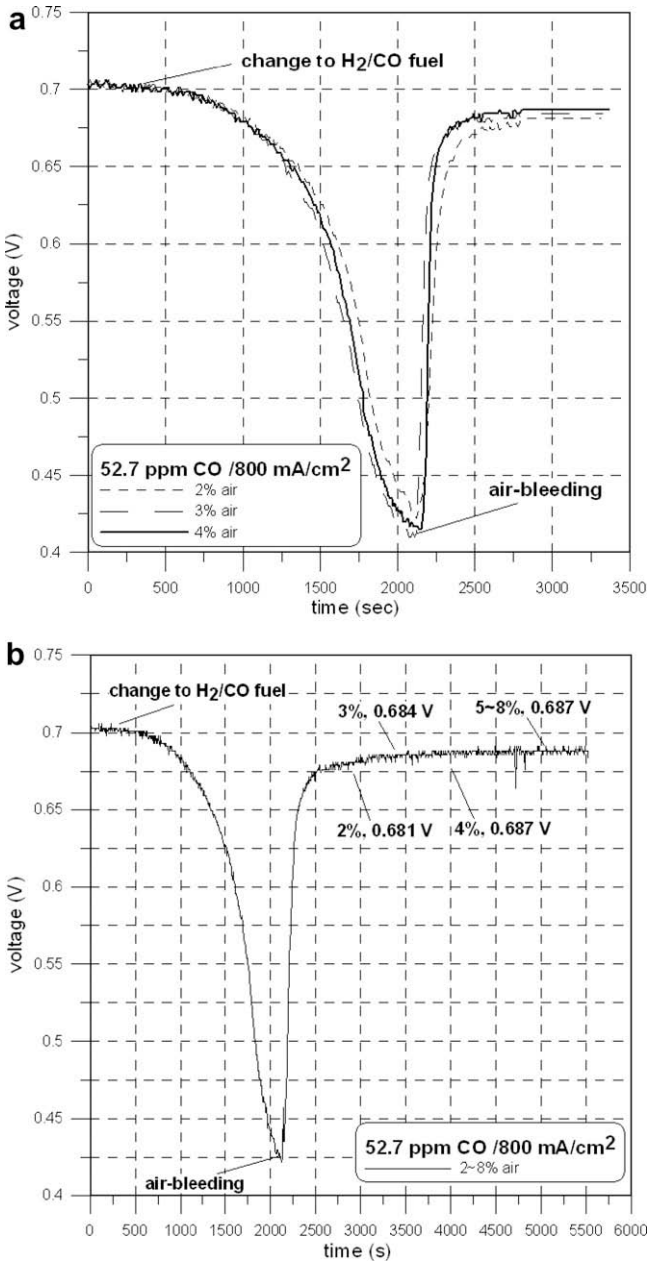

Fig. 7. (a) Cell voltage versus time and shows the cell voltage recovery for different air bleeding ratios (b) Curves for air bleeding ratios from 2% to 8%.

Thus, the optimum air ratio for bleeding was 4% for 52.7 ppm CO. This is because CO adsorption and desorption due to the presence of oxygen reach a steady state, and air ratios greater than 4% make no further contribution.

The majority of the O_2 consumed is for H_2 oxidation and only a small fraction is for CO oxidation. O_2 reacts with H_2 at the anode to produce H_2O. On the contrary, an air bleeding ratio greater than 8% may cause a decrease in cell performance. Excess O_2 lessens the amount of H_2 that can be oxidized on the catalyst surface. On the other hand, H_2 oxidation generates heat on the catalyst surface, which may destroy the anode catalyst and the cell membrane to cause a loss of cell performance. Thus, the air bleeding technique is useful in improving the CO tolerance, but a suitable air ratio is a critical factor.

Fig. 8 shows the steady polarization behaviors as a function of the air bleeding ratio after 30-min poisoning with 52.7 ppm CO. It is evident that an increase in air ratio from 2% to 4% increases

the cell performance. Comparison of the recovered polarization curves after air bleeding to that without air bleeding reveals a remarkable improvement in cell performance using this technique. The cell performance can recover to over 94% of the baseline level at the same current density using 4% air bleeding. The performance recovery rates for different current densities are also shown. For example, a recovery rate of 98% was obtained for 4% air bleeding at 800 mA/cm^2. However, the recovery rate was only 94.3% at 2000 mA/cm^2. At 2000 mA/cm^2 the baseline and recovery voltages were 0.544 V and 0.513 V, respectively. This is because the anode potential linearly increases with the cell current density and leads to different recovery rate at different current densities.

Two further CO concentrations were tested during 30-min poisoning experiments. The experimental procedures were the same as for 52.7 ppm CO.

Fig. 9 showed the corresponding steady state recovery polarization curves after air bleeding for 52.7, 25, and 10.1 ppm CO. For 10.1 ppm CO in the anode fuel stream, injection of 1.5% air yielded optimum CO tolerance for the fuel cell, with >97% recovery compared to the baseline level under the same current density. For 25 ppm CO, injection of 3% air into the anode fuel stream yielded optimum CO tolerance, with >96% recovery.

3.2.2. Short poisoning duration (3 min)

Experiments with 3-min CO poisoning were carried out using similar procedures to those for the 30-min poisoning, with the only difference being the poisoning duration. The previous 30-min CO poisoning experimental results showed that the optimum air bleeding ratios were 4% for 52.7 ppm CO, 3% for 25 ppm CO, and 1.5% for 10.1 ppm CO, respectively. Accordingly, air bleeding ratios were also tested from 4% to 1.5% in this 3-min CO poisoning case. However, the resultant performances of recovery rates for different air bleeding ratios were found insignificant among these experiments. Therefore, only the optimum air ratios for each CO concentration were presented in Fig. 10a–c.

Plots of cell voltage versus time were shown in Fig. 10a–c. The initial cell potential was 0.701 V at a current density of 800 mA/cm^2. Similar to that of Fig. 7, a baseline of pure hydrogen was constructed in the duration of initial 250 s, then, various concentrations of CO with hydrogen were fed to the anode. There was little if any decrease in cell voltage (0.698–0.701 V) for all CO concentration after 3 min of poisoning. Then air was injected into the anode fuel stream and the system reached a steady state approximately 20 min later. For 3% air bleeding, optimum CO tolerance was obtained when the anode fuel stream contained 52.7 ppm CO. The cell potential was 0.693 V at a current density of 800 mA/cm^2 and 98.9% of the baseline performance was recovered (Fig. 10a). Only 1.5% air was required for optimum CO tolerance (0.696 V) for 25 ppm CO, with 99.3% recovery of the cell potential (Fig. 10b). Owing to the limits of the air bleeding flow meter, the flow rate could not be set to less than 1% of full capacity (500 cm^3/min). Thus, to determine the optimum air bleeding ratio for 10.1 ppm CO, air bleeding in periodic mode was investigated. The air dosing duration was set to 10 s at intervals of 10 s. Periodic bleeding of 1.5% air yielded the best CO tolerance (0.697 V) in 3-min poisoning tests (Fig. 10c).

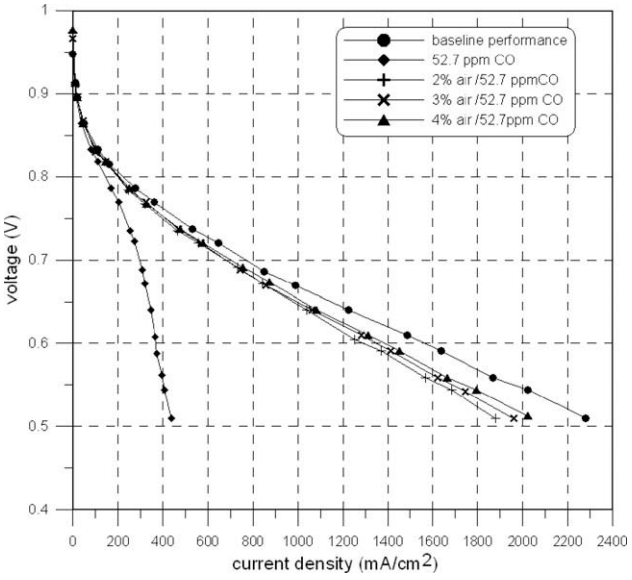

Fig. 8. The steady polarization behavior with different air bleeding ratios after 30 min 52.7 ppm CO poisoning.

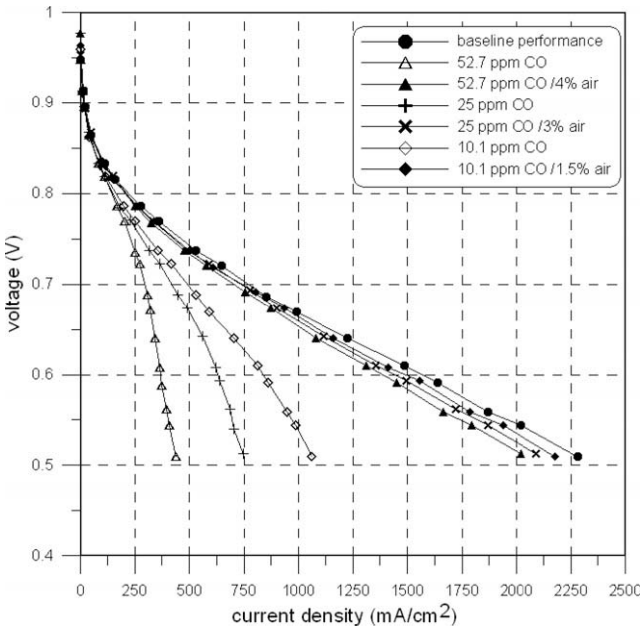

Fig. 9. The recovery polarization curves at steady state after air bleeding for 52.7, 25 and 10.1 ppm CO.

Fig. 11 shows steady state polarization curves after air bleeding during 3-min CO tests. It is evident that the CO tolerance can be effectively improved if air is introduced into the anode fuel stream in the initial poisoning stage (3 min). The cell performance could be recovered to >97% of the baseline level at the same current density. At the lower CO concentrations (10.1 and 25 ppm), the effect of CO poisoning can almost be completely abolished using the air bleeding technique.

3.3. Effect of different catalyst components

The effects of different anode catalysts (pure Pt and Pt–Ru alloy) on CO tolerance were investigated. Literature reports [4–7] indicate that Pt–Ru alloy catalysts yield better CO tolerance for fuel cells. In general, the anode catalyst in commercial MEAs is usually Pt–Ru alloy and the cathode catalyst is always pure Pt. Because the activity of oxygen is lower than that of hydrogen, a higher loading of Pt on the cathode is required for catalysis. A commercial Gore MEA was used as the fuel cell in the present study, with Pt–Ru and pure Pt loadings of 0.45 mg/cm^2 and 0.6 mg/cm^2, respectively. In the present study, we used pure Pt as the anode catalyst for comparison purposes. However, no such design is available in a commercial MEA. Therefore, we switched the cathode to the anode and vice versa, yielding Pt–Ru as the cathode catalyst and Pt as the anode catalyst. Under these conditions, the baseline performance is

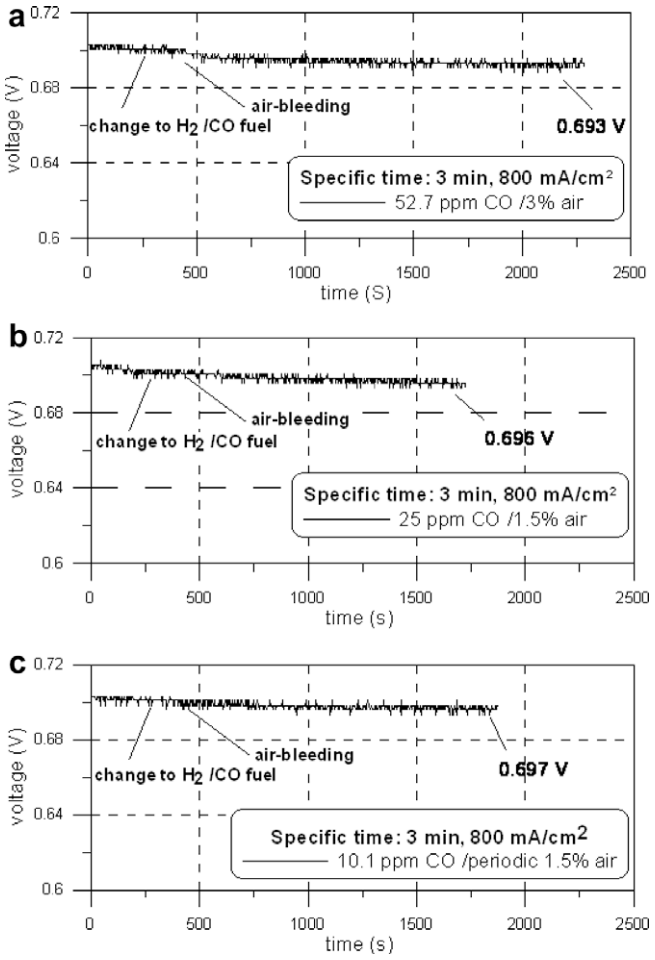

Fig. 10. (a), (b) and (c) Transient air bleeding tests for different CO poison concentrations (52.7, 25 and 10.1 ppm), the timing of air bleeding is 3 min.

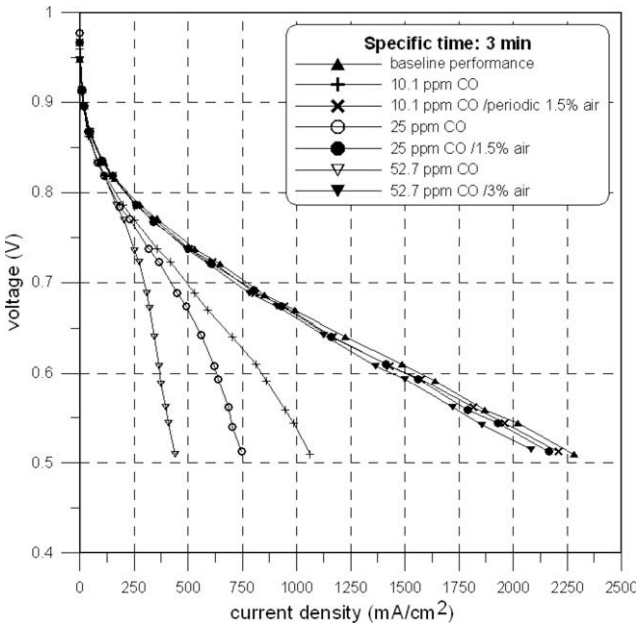

Fig. 11. Steady state polarization curves after air bleeding during 3 min.

expected to differ from that of the original configuration owing to the different loadings. This leads to difficulties in direct comparison of CO tolerances for the two cases. However, useful information can still be obtained for CO poisoning tests with and without air bleeding for the two configurations.

The procedure for CO poisoning tests was exactly the same as for the previous two sections. The cell current density was fixed at 800 mA/cm^2 and the anode was fed with pure hydrogen for the first 5 min, then changed to H_2/52.7 ppm CO. During these tests, the timing for air introduction was 35 min.

Fig. 12 showed curves for the Pt–Ru and Pt anode catalysts. The cell voltage decreased very quickly when CO was present in the anode fuel. The initial cell voltage was 0.701 and 0.657 V for the Pt–Ru and Pt anode catalysts, respectively. After switching the anode and cathode catalyst layers, the cathode loading was 0.45 mg/cm^2, which is less than the original loading of 0.6 mg/cm^2. The lower loading led to lower baseline performance and initial potential (0.657 V) during transient tests. In the original case with a Pt–Ru anode catalyst, a steady state was reached after 45 min during CO poisoning tests and the cell voltage decreased to 0.417 V (59.5%). In the switched case with a pure Pt anode, the voltage decreased to a stable poisoned value of 0.303 V (46%) after 47 min. Thus, the Pt–Ru anode catalyst exhibited better CO tolerance, with less of a decrease in cell voltage compared to the Pt anode (Fig. 12). Alloying with Ru decreases the adsorption of CO onto the Pt surface and catalyzes CO oxidation and removal from the Pt surface. Although the Pt–Ru catalyst can improve the CO tolerance of the fuel cell, the decrease in CO poisoning effect was not very significant. Even with Pt–Ru as the anode catalyst, the cell performance exhibited a substantial decrease on poisoning with 52.7 ppm CO, especially after 30-min poisoning. The anode fuel was changed back to pure H_2 when the CO poisoning effect reached a steady state. The curves in Fig. 12 indicate that the cell voltage recovered rapidly for both Pt and Pt–Ru anode catalysts because purging with H_2 changes the equilibrium. The Pt–Ru catalyst exhibited faster recovery of the cell voltage after purging with H_2, indicating that Pt–Ru can remove CO more effectively.

Fig. 13 shows steady state baseline, poisoned and recovery polarization curves for the two anode catalysts. The baseline polarization for the Pt anode catalyst is only 70% of that of the Pt–Ru, as previously explained. The poisoned polarization curve for the Pt

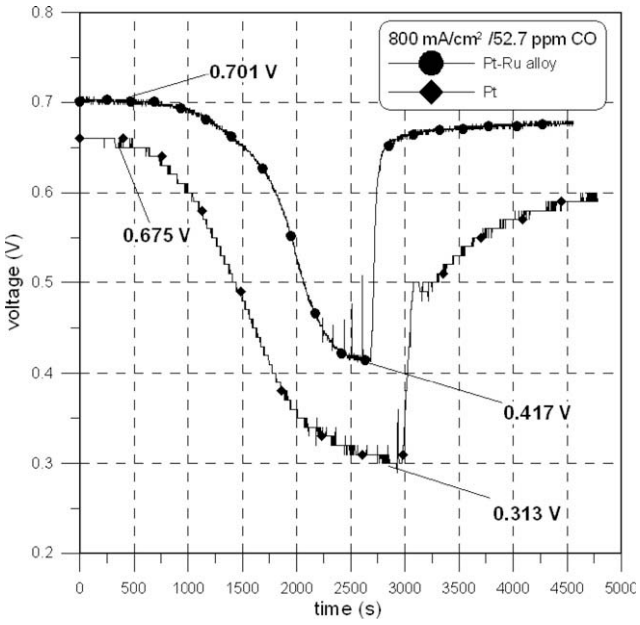

Fig. 12. Curves for the Pt–Ru and Pt anode catalysts.

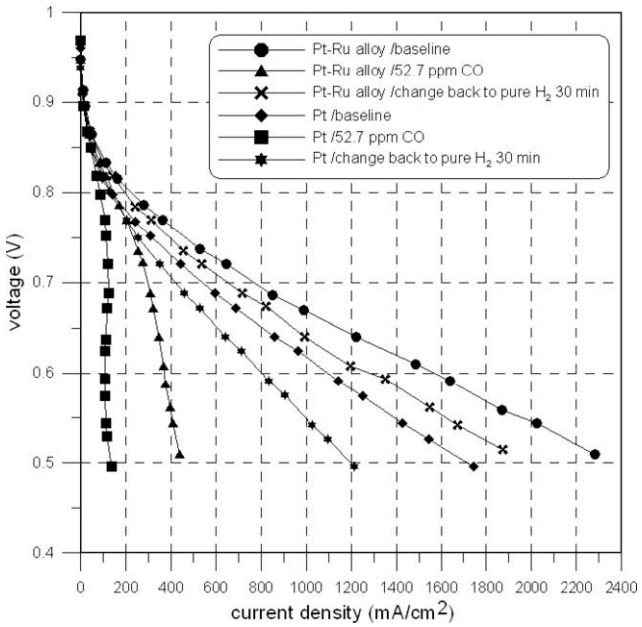

Fig. 13. Steady state baseline, poisoned and recovery polarization curves for the two different anode catalysts.

anode reveals a current density of only 137 mA/cm^2, which is less than 10% of the baseline performance (1744 mA/cm^2) at a cell voltage is 0.496 V. When the CO poisoning effect reaches a steady state, almost all of the active sites on the surface of the pure Pt catalyst are occupied by CO. The Pt–Ru catalyst exhibited better CO tolerance compared to the pure Pt catalyst. However, the cell performance was still only 20% (437 mA/cm^2) of the baseline value (2280.8 mA/cm^2) at a cell voltage of 0.51 V. There was an obvious recovery of cell performance after purging with pure H_2 for 30 min.

It has been verified that air bleeding can effectively improve the tolerance of the cell to 52.7 ppm CO for an anode catalyst of Pt–Ru. Fig. 14 shows transient curves for 52.7 ppm CO poisoning and air bleeding using pure Pt as the anode catalyst. CO (52.7 ppm) was

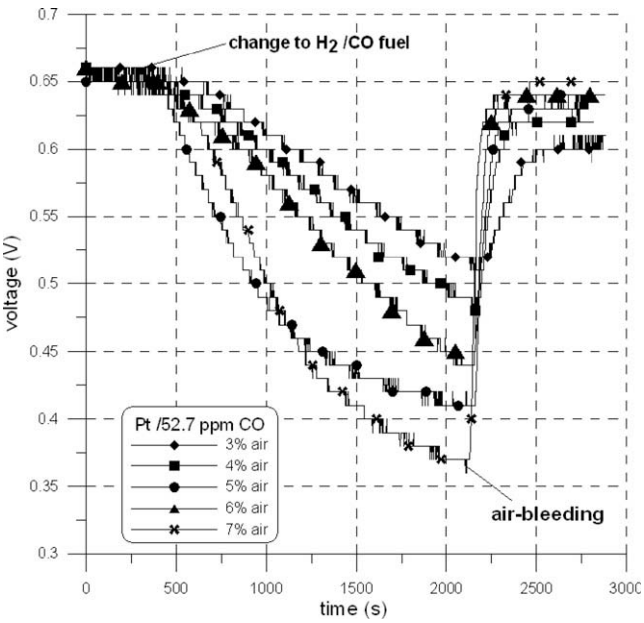

Fig. 14. Transient curves for 52.7 ppm CO poison and air bleeding using pure Pt as the anode catalyst.

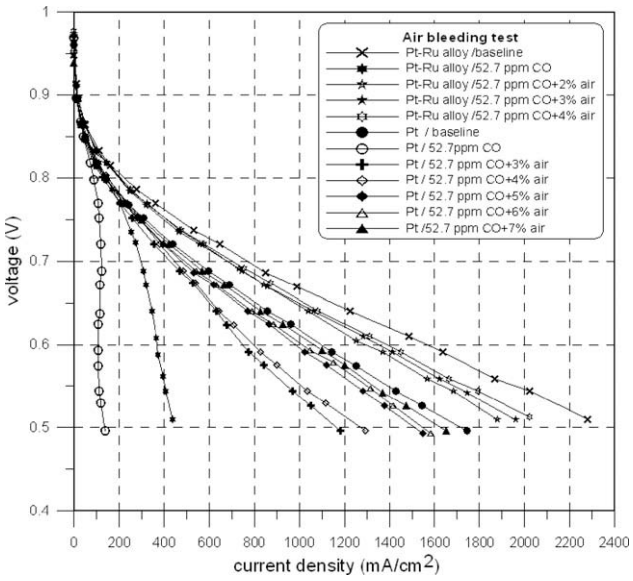

Fig. 15. Steady state polarization curves for different anode catalysts and the different concentrations of air bleeding.

introduced into the anode fuel stream after 5 min of pure H_2, then air is injected into the stream after 35 min of poisoning. It is evident that the cell voltage recovered quickly after air injection into the anode fuel stream. The cell exhibited optimum CO tolerance at a dose of 7% air and the cell voltage recovered to 0.649 V (98.8%) at a current density of 800 mA/cm^2. This demonstrates that air bleeding can increase the CO tolerance and improve the cell performance regardless of the type of anode catalyst (Pt or Pt–Ru). The Pt–Ru anode catalyst exhibited an optimum recovery rate of 98% when 4% air was introduced. The recovery rate was 98.8% with 7% air bleeding when the anode catalyst was pure Pt. This higher recovery can be attributed to the higher loading (0.6 mg/cm^2) for the Pt anode compared to the original (0.45 mg/cm^2), leading to greater O_2 adsorption and greater CO desorption from the Pt surface. Note that the poisoning rates were different for different poisoning durations, as explained in the previous section. However, the difference in poisoning rates was greater for pure Pt than for Pt–Ru at the anode catalyst. It was observed that the poisoning rate increased with the number of poisoning tests carried out. This may be because the interval between convective tests was too short and the catalyst properties may have changed after repeated poisoning experiments.

Fig. 15 shows the steady state polarization curves for different anode catalysts and the percentage of air bleeding. Without air bleeding the Pt–Ru anode catalyst exhibited better CO tolerance than the pure Pt catalyst. The air bleeding technique remarkably improved the CO tolerance for both Pt–Ru and pure Pt anode catalysts.

4. Conclusions

The study investigated that CO poisoning tests at a fixed current density. The results showed that a higher current density increased the cell CO tolerance. The anode potential reached the onset potential for CO oxidation at higher fixed current density, leading to CO removal from the Pt surface. The effects of air bleeding at different timings (3 and 30 min) during CO poisoning tests were also investigated for CO concentrations of 52.7, 25, and 10.1 ppm. Air bleeding technique improved successfully the cell CO tolerance and recovery of the poisoned performance regardless of the timing of the air introduction. Moreover, the effect of CO poisoning almost disappeared for

25 and 10.1 ppm CO. The effects of different catalysts (Pt–Ru alloy and pure Pt) on the cell performance during CO poisoning tests with and without air bleeding were investigated. Air bleeding could effectively increase the CO tolerance, regardless of the type of anode catalyst (pure Pt or Pt–Ru) used to perform CO poisoning tests.

Acknowledgement

The authors thank the National Science Council of the Republic of China, Taiwan, for financially supporting this research under Contract No. NSC 97-2221-E-009-067.

References

[1] M. Winter, R.J. Brodd, What are batteries, fuel cells, and supercapacitors, Chemical Reviews 104 (10) (2004) 4245–4269.
[2] H. Zhang, Y. Wang, E.R. Fachini, C.R. Cabrera, Electrochemically codeposited platinum/molybdenum oxide electrode for catalytic oxidation of methanol in acid solution, Electrochemical and Solid-State Letters 2 (1999) 437–439.
[3] H.P. Dhar, L.G. Christner, A.K. Kush, H.C. Maru, Nature of CO adsorption during H_2 oxidation in relation to modeling for CO poisoning of a fuel cell anode, Journal of the Electrochemical Society 134 (1987) 3021–3026.
[4] H.A. Gastiger, N.M. Markovic, P.N. Ross, E.J. Cairns, CO Electrooxidation on well-characterized Pt–Ru alloys, Journal of Physical Chemistry 98 (2) (1994) 617–625.
[5] H.A. Gastiger, N.M. Markovic, P.N. Ross, H_2 and CO Electrooxidation on well-characterized Pt, Ru, and Pt–Ru. 1. Rotating-disk electrode studies of the pure gases including temperature effects, Journal of Physical Chemistry 99 (20) (1995) 8290–8301.
[6] M. Watanabe, H. Igarashi, T. Fujino, Design of CO tolerant anode catalysts for polymer electrolyte fuel cells, Electrochemistry 67 (12) (1999) 1194–1196.
[7] E. Christoffersen, P. Liu, A. Ruban, H.L. Skriver, J.K. Noskov, Anode materials for low-temperature fuel cells: a density functional theory study, Journal of Catalysis 199 (2001) 123–131.
[8] H.A. Gastiger, N.M. Markovic, P.N. Ross, Electrooxidation of CO and H_2/CO mixtures on a well-characterized Pt_3 Sn electrode surface, Journal of Physical Chemistry 99 (1995) 8945–8949.
[9] S.J. Lee, S. Mukerjee, E.A. Ticianelli, J. McBreen, Electrocatalysis of CO tolerance in hydrogen oxidation reaction in PEM fuel cells, Electrochimica Acta 44 (1999) 3283–3293.
[10] B.N. Grgur, G. Zhuang, N.M. Markovic, P.N. Ross, Electrooxidation of H_2/CO mixtures on a well-characterized Pt_{75} Mo_{25} alloy surface, Journal of Physical Chemistry 101 (1997) 3910–3913.
[11] R.C. Urian, A.F. Gulla, S. Makerjee, Electrocatalysis of reformate tolerance in proton exchange membranes fuel cells: Part I, Journal of Electroanalytical Chemistry 554 (2003) 307–324.
[12] D.J. Ham, Y.K. Kim, S.H. Han, J.S. Lee, Pt/WC as an anode catalyst for PEMFC: activity and CO tolerance, Catalysis Today 132 (2008) 117–122.
[13] S. Gottesfeld, J. Pafford, A new approach to the problem of carbon monoxide poisoning in fuel cells operating at low temperatures, Journal of the Electrochemical Society 135 (1988) 2651–2652.
[14] L. Gubler, G.G. Scherer, A. Wokaun, Effects of cell and electrode design on the CO tolerance of polymer electrolyte fuel cells, Physical Chemistry Chemical Physics 3 (2001) 325–329.
[15] F.A. Uribe, J.A. Valerio, F.H. Garzon, T.A. Zawodzinski, PEMFC reconfigured anodes for enhancing CO tolerance with air bleed, Electrochemical and Solid-State Letters 7 (2004) 376–379.
[16] W. Shi, M. Hou, Z. Shao, J. Hu, Z. Hou, P. Ming, B. Yi, A novel proton exchange membrane fuel cell anode for enhancing CO tolerance, Journal of Power Sources 174 (2007) 164–169.
[17] H.S. Chu, F. Tsau, Y.Y. Yan, K.L. Hsueh, F.L. Chen, The development of a small PEMFC combined heat and power system, Journal of Power Sources 176 (2008) 499–514.
[18] C.H. Chen, C.C. Chung, H.H. Lin, Y.Y. Yan, Improvement of CO tolerance of proton exchange membrane fuel cell by an air-bleeding technique, Journal of Fuel Cell Science and Technology 5 (2008) 1–5.